arXiv:2509.04376v2 [cs.CV] 5 Sep 2025

ANOMALYLMM: BRIDGING GENERATIVE KNOWLEDGE AND DISCRIMINATIVE RETRIEVAL FOR TEXT-BASED PERSON ANOMALY SEARCH

Hao Ju[1] **Hu Zhang**[2] **Zhedong Zheng**[1†]
[1]Faculty of Science and Technology and Institute of Collaborative Innovation, University of Macau
[2]CSIRO Data61
{yc47429,zhedongzheng}@um.edu.mo, hu1.zhang@csiro.au

ABSTRACT

With growing public safety demands, text-based person anomaly search has emerged as a critical task, aiming to retrieve individuals with abnormal behaviors via natural language descriptions. Unlike conventional person search, this task presents two unique challenges: (1) fine-grained cross-modal alignment between textual anomalies and visual behaviors, and (2) anomaly recognition under sparse real-world samples. While Large Multi-modal Models (LMMs) excel in multi-modal understanding, their potential for fine-grained anomaly retrieval remains underexplored, hindered by: (1) a domain gap between generative knowledge and discriminative retrieval, and (2) the absence of efficient adaptation strategies for deployment. In this work, we propose AnomalyLMM, the first framework that harnesses LMMs for text-based person anomaly search. Our key contributions are: (1) **A novel coarse-to-fine pipeline** integrating LMMs to bridge generative world knowledge with retrieval-centric anomaly detection; (2) **A training-free adaptation cookbook** featuring masked cross-modal prompting, behavioral saliency prediction, and knowledge-aware re-ranking, enabling zero-shot focus on subtle anomaly cues. As the first study to explore LMMs for this task, we conduct a rigorous evaluation on the PAB dataset, the only publicly available benchmark for text-based person anomaly search, with its curated real-world anomalies covering diverse scenarios (*e.g.*, falling, collision, and being hit). Experiments show the effectiveness of the proposed method, surpassing the competitive baseline by $+0.96\%$ Recall@1 accuracy. Notably, our method reveals interpretable alignment between textual anomalies and visual behaviors, validated via qualitative analysis. Our code and models will be released for future research.

1 INTRODUCTION

Ensuring public safety is a growing priority in smart surveillance systems, driving the need for efficient text-based person anomaly search, a task that retrieves individuals exhibiting abnormal behaviors using natural language queries. Unlike generic text-based person search Zheng et al. (2020); Yang et al. (2023), this task focuses on identifying subtle, often rare anomalous actions (*e.g.*, falling, collision, or being hit) described in text. Such capability is critical for real-world applications, from crime prevention to emergency response. However, it remains underexplored due to the lack of dedicated benchmarks and the inherent complexity of aligning textual descriptions with fine-grained anomalous behaviors in videos.

This task introduces two key challenges: **(1) Fine-grained cross-modal alignment:** Anomalies are often described with nuanced semantics (*e.g.*, "staggering while clutching their chest"), requiring precise localization of transient visual cues. Existing methods Yang et al. (2024b); Zeng et al. (2024) struggle with such alignment, as they primarily focus on coarse-grained attributes (*e.g.*, clothing or pose). **(2) Sparse anomaly samples:** Real-world anomalies are sparse and diverse, making it challenging to train or fine-tune models effectively. While recent Large Multi-modal Models (LMMs) Li et al. (2023); Alayrac et al. (2022); Achiam et al. (2023); Yang et al. (2024a) show

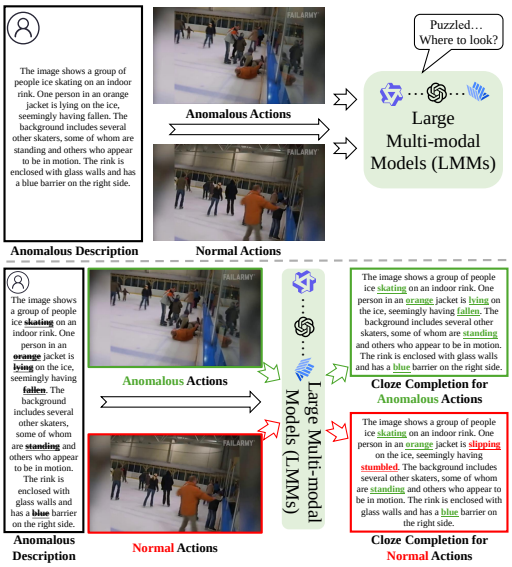

Figure 1: Motivation of AnomalyLMM. (Top) Direct retrieval of candidates with anomalous actions is challenging for Large Multi-modal Models (LMMs), due to the domain gap and long-tail anomaly recognition. (Bottom) Cloze completion is an effective adaptation strategy for LMMs, allowing LMMs to focus on relevant objects and establish fine-grained cross-modal alignment between text and images. Green completions in the bottom-right box indicate that completions from LMM align with the anomalous description, while red completions denote mismatches.

strong general-purpose visual-language reasoning, they are primarily designed for generative tasks rather than discriminative retrieval. Consequently, there exists a notable domain gap between their pretraining objectives and the specific demands of anomaly retrieval. Moreover, there remains a lack of efficient adaptation strategies to effectively leverage LMMs for deployment in few-shot or resource-constrained scenarios, limiting their applicability to real-world surveillance tasks (see Figure 1 (Top)).

In this work, we propose AnomalyLMM, the first framework that strategically adapts LMMs for text-based person anomaly retrieval. Instead of directly relying on LMMs to retrieve images based on the given text query, we propose a coarse-to-fine retrieval pipeline that first narrows the candidate space and then progressively refines the search using LMMs' reasoning abilities. Specifically, we first employ a pre-trained text-to-image retrieval model to produce an initial list of candidate images given a natural language anomaly query. These models, trained for global cross-modal alignment, are efficient at coarse-level retrieval and serve as a strong foundation for subsequent reasoning.

To move beyond coarse retrieval and enable more fine-grained alignment, we reformulate anomaly search as a masked cloze-style reasoning task. Key verbs and color attributes in the original query are replaced with structured placeholders (`< VERB >`, `< COLOR >`) using an LLM. This yields a masked query that disentangles action semantics and visual appearance, prompting the model to focus on specific anomaly-related cues. Each candidate image is then paired with the masked query and fed into an LMM. We argue that only the ground-truth image could provide the visual cues to generate the accurate verb and color words, while others are challenging to fill all cloze questions. The model is instructed to fill in the placeholders based on visual evidence. This cloze-style completion transforms each candidate frame into a query-specific textual description. To avoid hallucinations, we constrain the LMM to output `UNKNOWN` when uncertain, ensuring that completions are grounded in the image. Finally, the original query is compared with all image-specific completions using an LLM. This comparison is performed semantically, considering language variability. Verbs with similar meanings (*e.g.*, "balancing" and "sliding") or colors with close hues (*e.g.*, "dark" and "gray") are treated as matched. Based on the number of matched placeholders, a re-ranking is performed.

To obtain the final ranking, we combine the initial ranking list with a semantically obtained re-ranking list using a score fusion strategy. Together, these steps form a unified pipeline that reformulates the anomaly retrieval task as a masked completion and re-ranking process. AnomalyLMM enables LMMs to operate in a reasoning-centric fashion without requiring additional training or fine-tuning. Our work delivers three primary contributions as follows:

- **A coarse-to-fine retrieval pipeline** that synergizes LMMs' generative knowledge with discriminative anomaly detection, addressing the domain gap through retrieval-centric alignment.
- **A training-free adaptation cookbook** featuring masked cross-modal prompting to highlight anomaly-specific cues, behavioral saliency prediction for sparse visual localization, and knowledge-aware re-ranking to refine retrieval with world knowledge.
- **Rigorous benchmarking on the PAB dataset Yang et al. (2024b)**, the only public benchmark for this task, where our method outperforms baselines by 0.96% Recall@1 accuracy and shows interpretable anomaly-behavior alignment via qualitative analysis.

The rest of this paper is organized as follows. Section 2 reviews related works. Section 3 describes the proposed AnnolyLMM framework in detail. Experimental results and comparisons are discussed in Section 4, followed by conclusions in Section 5.

2 Related Work

Here we briefly review the three most relevant topics, *i.e.*, anomaly detection in public safety, fine-grained cross-modal retrieval, and large multi-modal models for discriminative tasks.

2.1 Anomaly Detection in Public Safety

Traditional anomaly detection approaches rely on handcrafted features Wang & Miao (2010) or reconstruction-based paradigms Hasan et al. (2016), identifying anomalies as statistical deviations from learned normal patterns. Recent advances adopt deep learning for spatio-temporal modeling, including graph networks Scarselli et al. (2008) for crowd dynamics and self-supervised learning Gui et al. (2024) to exploit unlabeled behavioral data. While methods Sultani et al. (2018) achieve strong video-level anomaly classification, they operate in an unsupervised manner, lacking explicit mechanisms to align visual anomalies with textual queries. Following the general person re-identification Zheng et al. (2017) and text-guided person search Zheng et al. (2020); Bai et al. (2023), text-anchored approaches Shen et al. (2023); Wang et al. (2025) attempt cross-modal retrieval but face two limitations: (1) coarse-grained semantics such as the binary tags (normal/abnormal). Such annotation limitation overlooks subtle behavioral cues (*e.g.*, *staggering* vs. *falling*), and (2) bias toward normal behaviors due to long-tail distributions. The system learns more normal behaviors, and is prone to predict normal actions. To address the data scarcity, Yang *et al.*introduce the PAB dataset Yang et al. (2024b) that pioneers text-based person anomaly search to cover more anomaly action types via natural language description, yet state-of-the-art solutions Zeng et al. (2024); Yang et al. (2024b) rely on supervised fine-tuning, which struggles with rare or unseen anomalies. Therefore, it remains challenging to design a scalable system for unseen anomaly actions and give quick responses, which is a key to smart city management. In an attempt to general anomaly detection system, our work addresses these gaps by unifying generative knowledge from LMM and LMM with discriminative retrieval.

2.2 Fine-Grained Cross-Modal Retrieval

Fine-Grained Cross-Modal Retrieval has gained increasing attention due to its ability to align and retrieve highly specific content across different modalities (*e.g.*, images and text). Early works in cross-modal retrieval primarily focused on coarse-grained alignment, learning shared representations using methods like Canonical Correlation Analysis (CCA) Andrew et al. (2013) and deep metric learning Lu et al. (2017). However, these approaches often struggle with fine-grained distinctions due to their limited ability to capture subtle inter-modal correspondences. Recent advances leverage fine-grained feature interactions to improve retrieval precision. For instance, Faghri et al. (2018)

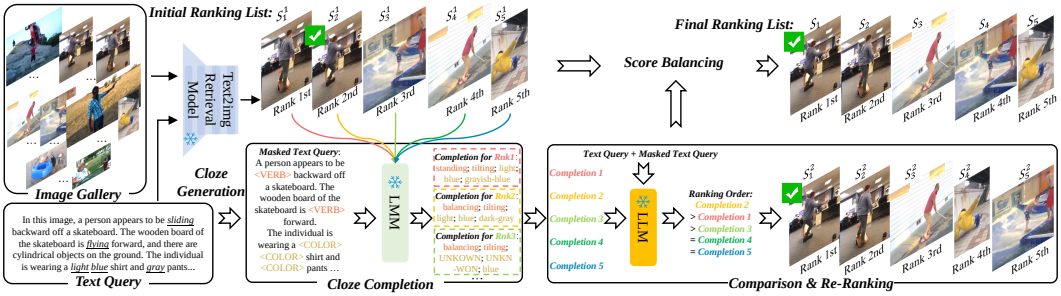

Figure 2: *Overall pipeline of the proposed AnomalyLMM.* First, given a text query about the target person with anomaly action, we apply an off-the-shelf text2image retrieval model to obtain the initial ranking list (*left*). Next, the verbs and colors in the text query are replaced with placeholder tokens ¡VERB¿ and ¡COLOR¿ via a pre-trained LLM, generating clozes (*Cloze Generation*). According to the candidate images, a pre-trained LMM is then prompted to complete these clozes by predicting masked tokens for each image in the initial ranking list (*Cloze Completion*). We argue that only the ground-truth image could provide the visual cues to generate the accurate verb and color words, while others are challenging to fill all cloze questions. Subsequently, the completions for each image are compared and re-ranked by an LLM in a semantic equivalent manner, producing the re-ranking list (*Comparison & Re-Ranking*). Finally, the initial and re-ranking lists are combined through score balancing to produce the final ranking list (*upper-right*).

introduces a hierarchical alignment framework that matches local regions in images with phrases in text, while Ji et al. (2021) employs cross-modal attention to dynamically focus on discriminative sub-elements. Transformer-based models Gorti et al. (2022) further enhance fine-grained retrieval by modeling long-range dependencies across modalities. Another line of research explores contrastive learning for fine-grained cross-modal alignment. Methods like Radford et al. (2021) employ instance- and patch-level contrastive losses to enforce both global and local consistency. Additionally, Dong *et al.* Dong et al. (2021) proposes a graph-based reasoning approach to model fine-grained relationships between visual and textual entities explicitly. Despite progress, challenges remain in handling highly nuanced queries and mitigating modality-specific biases. Our work addresses these limitations by introducing a training-free cross-modal re-ranking mechanism that enhances fine-grained discriminability while maintaining computational efficiency.

2.3 Large Multi-modal Models for Discriminative Tasks

Recent LMMs Chen et al. (2024b); Yao et al. (2024) unify vision-language understanding through large-scale pre-training on aligned image-text pairs. Some works also explore audio Deshmukh et al. (2023), video Maaz et al. (2023); Chen et al. (2024a) and multiple data formats Wu et al. (2024). The typical models like CLIP Radford et al. (2021), BLIP Li et al. (2023) based on contrastive learning enable zero-shot cross-modal retrieval, while generative LMMs (*e.g.*, GPT-4V 202 (2023), LLaVA Liu et al. (2023)) excel in open-world reasoning via instruction tuning. However, adapting these models for fine-grained anomaly search poses unique challenges as follows. (1) *Semantic Granularity Gap.* Generative LMMs prioritize holistic scene understanding over localized behavioral anomalies Radford et al. (2021); (2) *Adaptation Inefficiency.* Existing strategies Zhang et al. (2023); Rong et al. (2025) require full fine-tuning or adding additional parameters for tuning, such as LoRA Hu et al. (2022) and WoRA Sun et al. (2025), which are still prohibitively expensive for sparse anomaly data and large GPU memory consumption. While prompt-based methods Zhou et al. (2022) improve attribute alignment, they fail to capture dynamic anomaly saliency (*e.g.*, temporal *collision* cues). Our framework innovates by (i) repurposing LMMs' world knowledge for anomaly localization without parameter updates, and (ii) introducing a training-free adaptation protocol to bridge generative and discriminative paradigms.

(a) Prompt for cloze generation

You are a linguistic analyzer. Your task is to extract all verbs and verb phrases from the input sentence.

Steps:
1. Identify all meaningful verbs and verb phrases for actions, ignoring auxiliary/modal verbs.
2. Exclude any non-verb words from verb phrases, including nouns, adjectives, adverbs, prepositions, and pronouns.
3. Phrasal verbs: Only include the verb in a phrasal verb, and exclude any prepositions or nouns.
4. Exclude any words or phrases that do not describe an action.

Examples:
…

(b) Prompt for cloze completion

Based on the VISUAL EVIDENCE in the image, replace each <VERB> and <COLOR> slot in the given template with exactly one contextually appropriate word.

Think following these steps:
1. Analyze the subjects' body positions, spatial relationships, and environmental context in the input image.
2. Identify only the observable actions or colors supported strictly by visual cues (\eg limb angles, movement, color visible in the image).
3. Do NOT guess or infer any information from the input text or external knowledge.
4. If no visual evidence supports a replacement, or if the described objects do not appear in the image, use the word 'UNKNOWN' for that slot.

Examples:
…

(c) Prompt for comparison & re-ranking

Background:
There are three types of inputs:
1. A template sentence that contains <COLOR> and/or <VERB> placeholders.
2. A description that fills those placeholders.
3. N options (labelled A, B, C …). Each option is a sentence that also fills the placeholders.

Treat all inputs as visual descriptions of images.

Task:
Rank the options by how well their replacement words for each placeholder match those in the description. Count both exact and visually / functionally equivalent matches.

Equivalence rules:
<COLOR>:
1. Same hue or obvious tint/shade is equivalent.
2. Near-hue neighbors count as matches.
3. Distinct hues are not equivalent.

<VERB>:
1. Evaluate the visible action, not the literal wording.
2. Two verbs are equivalent when they depict the same physical motion and the same state/instability.
3. Do not favor exact lexical matches over visually equivalent verbs.

Examples:
…

Figure 3: *Prompt for different steps in AnomalyLMM.* (a) Prompt for cloze generation. This prompt is designed for the LLM to extract verbs that describe actions from input sentences. A similar prompt is used for identifying color-related descriptions. (b) Prompt for cloze completion. This prompt guides the LMM to use visual evidence from images to fill the ¡VERB¿ and ¡COLOR¿ tokens in the masked text query with contextually appropriate words or 'UNKNOWN' when no visual support exists. (c) Prompt for comparison & re-ranking. This prompt directs the LLM to compare and rank the generated completions based on semantic equivalent rules, considering both exact and visually/functionally similar matches.

3 METHODOLOGY

Our method begins with a coarse-to-fine retrieval pipeline. We first leverage an off-the-shelf text-to-image retrieval model to produce an initial ranking of candidate frames. This is followed by three key steps: Cloze Generation, Cloze Completion, and Comparison & Re-ranking. The final ranking result is obtained by fusing the initial ranking list with the re-ranking result. A brief overview of the pipeline is shown in Figure 2. We are inspired by the cloze task to bridge the gap between the large models pretrained on generative tasks to the discriminative retrieval demands. We argue that only the ground-truth image could provide the visual cues to generate the accurate verb and color words, while others are challenging to fill all cloze questions. **In this work, we do not pursue the best text-to-image model for coarse retrieval, but focus on further improvement by leveraging large models to narrow down the final candidate ranges.**

3.1 INITIAL RANKING GENERATION

We adopt a coarse-to-fine strategy starting with an initial filtering step. Specifically, we employ a dedicated text-to-image retrieval model, *i.e.*, X^2VLM. This model is trained to match visual content with natural language descriptions and has been widely used in general retrieval tasks due to its efficiency and discriminative power. Given a natural language anomaly query, we retrieve the top-N images from the dataset. These candidates form an initial ranking list which is expected to include both relevant and irrelevant results. By reducing the input space for subsequent processing, we not only improve computational efficiency but also allow the LMM to operate in a more focused, context-rich setting. This design reflects a deliberate strategy to bridge the gap between LMMs' generative world knowledge and retrieval-centric anomaly detection. While Large Multi-modal Models (LMMs) excel at contextual reasoning and text-image generation, their native formulation is not

directly optimized for discriminative retrieval tasks. In contrast, text-to-image retrieval models are specifically trained to align visual and textual features for ranking, making them well-suited for initial coarse-level candidate selection. Instead of directly aligning the text query with visual content using LMMs, we first convert the images in the initial ranking list into text descriptions via cloze generation and completion. This allows us to perform the comparison entirely in the textual domain by matching the generated descriptions with the original query.

3.2 CLOZE GENERATION

We leverage Large Language Models (LLMs) to generate two distinct types of masks from the input text query: verb masks and color masks. These masks are designed to disentangle action semantics and appearance attributes, enabling the model to focus more effectively on salient cues relevant to anomaly retrieval. For the verb mask, we utilize an LLM (e.g., *QVQ-Max*) to identify all action-related or lexical verbs within the query. Each detected verb is then replaced with a standardized placeholder token, `< VERB >`. For the color mask, we prompt the same LLM to extract all color-related descriptions that refer to either the person or their surrounding environment. Identified color terms are similarly substituted with `< COLOR >` tokens one by one. The specific prompts used for action-related verbs are illustrated in Figure 3 (a) (The prompt for color-related descriptions is also similar). By combining these two types of masks, we obtain a masked text query, which serves as part of the input to the LMM in the subsequent anomaly-aware retrieval process.

3.3 CLOZE COMPLETION

Given a masked text query containing structured placeholders, *i.e.*, $<\text{VERB}>$ and $<\text{COLOR}>$, we employ an LMM to perform cloze-style completion for each image in the initially retrieved ranking list. Specifically, for each candidate image in the ranking list, the LMM is prompted with the image and the obtained masked query as context, and tasked with filling in the missing placeholders based on visual evidence. This process is repeated for all N images in the initial ranking list, resulting in N distinct cloze completions tailored to the visual content of each image. To avoid hallucinated completions, we explicitly instruct the LMM to output ``UNKNOWN'' if it cannot confidently infer the placeholder content from the given image. Meanwhile, this constraint also helps alleviate the tendency of generating context-independent completions solely based on textual priors rather than grounding them in visual evidence. An example prompt used for this cloze completion step is illustrated in Figure 3 (b). These completions are then used for fine-grained re-ranking in the next step.

3.4 COMPARISON & RE-RANKING

Comparison. Each image in the initial ranking list is associated with a cloze completion generated from the masked query. To assess the relevance of each image, we compare its completion with the original text query using an LLM-based semantic comparison. Specifically, the LLM receives three inputs: the original query, the masked query (with placeholders), and the set of generated completions. By including the masked query, we guide the LLM to focus on the replaced tokens, enabling a more targeted comparison at the locations of interest. Given the inherent ambiguity and variability in natural language, we perform semantic rather than literal comparison. That is, instead of checking for exact word matches, we evaluate whether the generated completions convey concepts consistent with those in the original query. For verbs, actions that are semantically similar (*e.g.*, "balancing" vs. "sliding") are treated as matched when they describe equivalent behaviors, such as a person on a skateboard poised to slide. Similarly, color terms like "gray" and "dark" are treated as equivalent when referring to the same clothing item. This semantic alignment helps ensure that images are ranked not only by surface-level similarity but by conceptual consistency with the original text query.

Re-Ranking. Following the semantic comparison, we prompt the LLM to re-rank all completions in descending order based on the number of semantically matched placeholder substitutions. To account for cases where multiple completions exhibit the same level of semantic consistency with the original query, we also instruct the LLM to identify equivalence relationships during re-ranking. In such cases, completions with equal semantic alignment are assigned the same rank. The full prompt used for semantic comparison and re-ranking is provided in Figure 3 (c). To obtain the final

ranking result, we combine the rankings from the initial ranking list and the re-ranking result. The initial ranking is based on the retrieval scores predicted by the text-to-image model, whereas the re-ranking result is based purely on semantic alignment and provides only an ordered list without associated scores. To enable fusion across the two lists, we assign scores to the re-ranking result using an exponential decay function with base β. Specifically, for a completion ranked at position n, its score is computed as: $S_n^2 = \beta^n$. The final ranking score is then computed as a weighted combination of the two lists:

$$S_n = \alpha_1 S_n^1 + \alpha_2 S_n^2, \quad n \in [0, N-1], \tag{1}$$

where α_1 and α_2 are balancing weights, S_n^1 and S_n^2 represent the scores from the initial and re-ranking lists, respectively, and N is the number of retrieved candidates in the initial list. We note that there are some corner cases. If LLM could not justify whether the candidate is better, it could select that the answers of the two candidates are equally correct. In this case, we will rely more on the initial ranking result.

Discussion-1. What are the advantages of cloze generation and completion? Inspired by recent successes in general text-based person retrieval Niu et al. (2025); Tan et al. (2024); He et al. (2024) and target region localization in LMMs Zhang et al. (2025); Liu et al. (2024), we propose cloze generation and completion to better exploit the reasoning capabilities of LMMs and guide their attention toward anomalous regions in the image. Compared with previous methods, our cloze generation and completion offer two key advantages: (i) Both modules are *training-free* and do not require any additional training or fine-tuning, making them efficient and effective for text-based person anomaly search, especially since real-world anomaly data is scarce and insufficient for fully training LMMs; (ii) Cloze generation and completion actively prompt LMMs to infer missing information based on both the image content and the surrounding textual context. This naturally encourages the model to attend to visually relevant regions aligned with the anomaly description, enhancing interpretability and retrieval precision.

Discussion-2. What are the advantages of comparison & re-ranking? The proposed comparison & re-ranking method has three advantages. (1) Precise alignment between text query and visual content is critical for anomaly search. Instead of fusing cross-modal features, our method compares cloze completions in the textual domain, enabling fine-grained, interpretable alignment that fully leverages the language understanding capabilities of LLMs. (2) Due to the inherent ambiguity in natural language, identical actions can be described using different words. Instead of surface-level or lexical matching, our module performs comparison in a semantically equivalent manner, making it more robust to diverse phrasings of the same concept. (3) Unlike methods that predict absolute similarity scores Zeng et al. (2024; 2022), we focus on comparing and directly predicting the relative ranking. By restricting comparison to masked positions (*e.g.*, verbs, colors) and jointly considering all candidates in the initial list, the LLM benefits from global context to make more consistent and context-aware reordering decisions.

4 EXPERIMENT

In this section, we elaborate on the implementation details, comparison with competitive methods, ablation studies with different LLMs and LMMs, and further discussion. We note that our method is compatible with existing methods to further improve the performance.

4.1 IMPLEMENTATION DETAILS

Dataset. Pedestrian Anomaly Behavior (PAB) dataset Yang et al. (2024b) is the first large-scale benchmark for the text-based pedestrian anomaly search, covering diverse scenarios (*e.g.*, running, performing, playing soccer, ice-skating) paired with their anomalous counterparts (*e.g.*, lying, being hit, falling, lying) for the same identity. PAB includes a large-scale training set with 1,013,605 synthesized image-text pairs (normal and anomalous) generated via a diffusion-based pipeline Rombach et al. (2022) to ensure fine-grained text-visual alignment Yang et al. (2024b). The test set contains 1,978 real-world image-text pairs with manually verified anomalies, providing a rigorous evaluation platform.

Evaluation Metrics. We adopt standard retrieval metrics. Mean Average Precision (mAP) is used to measure overall ranking quality by averaging precision across recall thresholds, emphasizing correct

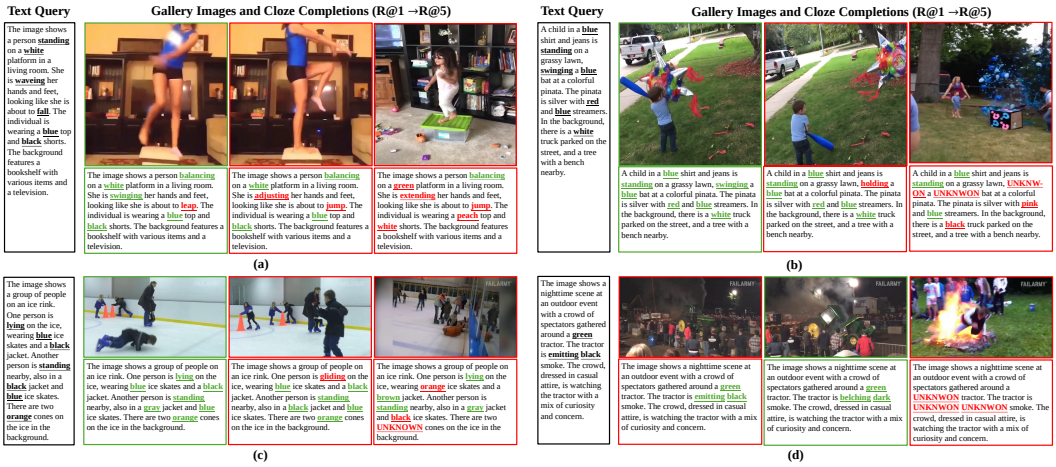

Figure 4: Qualitative results on the PAB dataset Yang et al. (2024b). (a)-(c): successful cases; (d): a failure case. Given text queries (left), matched gallery images and cloze completions are in green, and mismatched are in red (right). In (c), the presence of highly similar objects exhibiting comparable appearances and actions consistent with the query text results in a reasonable failure. Zoom in for a better visualization.

top-rank retrievals. Recall@K computes the fraction of queries where the true match appears in the top-K results, reflecting real-world usability. We mainly report the Recall@1 (R@1) considering the fine-grained retrieval demands.

Training Details. Most of the proposed method is training-free, and we only fine-tune the text-to-image retrieval model on the PAB dataset Yang et al. (2024b). We adopt X^2VLM Zeng et al. (2024) as the text2image retrieval model, initializing it with pre-trained weights and fine-tuning it on the PAB dataset. The model is fine-tuned with a batch size of 22 using the AdamW optimizer Loshchilov & Hutter (2019) and a weight decay of 1×10^{-2}. The starting learning rate is set to 5×10^{-5} and scheduled by a StepLR policy, with a warmup of 5×10^3 iterations and decays applied at 2×10^4 and 3.5×10^4 iterations.

Table 1: Comparison of proposed method with competitive methods on the PAB dataset. Integrating representative text-to-image retrieval models into the proposed method consistently improves performance. Both CMP and X^2VLM benefit from notable gains in Recall@1 (R@1) and mAP when combined with our approach.

Method	R@1	mAP
APTM	72.14	82.78
IRRA	76.39	86.33
CLIP	77.60	87.35
RaSa	80.79	89.20
X-VLM	81.95	89.86
CMP	69.51	81.06
CMP + *Ours*	73.15 (+3.64)	83.64 (+2.58)
X^2VLM	83.77	90.43
X^2VLM + *Ours*	**84.73 (+0.96)**	**90.89 (+0.46)**

4.2 Comparison with Competitive Methods

Quantitative Results. We incorporate two representative methods, *i.e.*, CMP and X^2VLM, as the text-to-image retrieval model in AnomalyLMM and evaluate their performance against other competitive approaches (see Table 1). All competitive methods are fine-tuned on the PAB dataset Yang et al. (2024b). The proposed method achieves notable improvements over strong baselines Yang et al. (2024b); Zeng et al. (2024). Specifically, we observe $+3.64\%$ Recall@1 accuracy, $+2.58$ mAP on CMP baseline, and $+0.96\%$ Recall@1 accuracy, $+0.46$ mAP on X^2VLM baseline. These results validate the effectiveness of cloze generation, completion, and comparison & re-ranking in the proposed method and facilitate the text-based person anomaly search.

Table 2: Ablation studies. (a) Ablation study of primary components. Applying both yields the best performance. (b) Ablation study of weighting strategies for re-ranking. Exponential decay with base 0.5 achieves the best performance. (c) Ablation study of LLM or LMM for different steps. (d) Ablation study on the number of initial candidates. A length of three achieves the best performance. (e, f) Ablation study of hyper-parameters (α_1, α_2) for score balancing.

(a)

Method	Cloze Gen. & Completion	Comparison & Re-Ranking	R@1	mAP
Baseline	✗	✗	83.77	90.43
w Cloze Completion	✓	✗	84.12	90.60
w Re-Ranking	✗	✓	84.22	90.65
Ours	✓	✓	**84.73**	**90.89**

(b)

Strategy	Hyper-parameter	Performance	
		R@1	mAP
Exponential β	0.70	84.63	90.86
	0.50	**84.73**	**90.89**
	0.30	84.73	90.88
	0.20	84.68	90.88
Linear d	-0.30	84.68	90.88
	-0.20	84.73	90.88
	-0.10	84.68	90.88

(c)

LLM/LMM Selection			Performance	
Cloze Gen.	Cloze Comp.	Re-Ranking	R@1	mAP
QWQ-Max	QVQ-Max	Qwen2.5-3B	83.67	90.37
QWQ-Max	QVQ-Max	Qwen2.5-7B	83.87	90.48
QWQ-Max	Qwen2.5-VL-7B	QWQ-Max	84.13	90.62
QWQ-Max	Qwen2.5-VL-3B	QWQ-Max	84.22	90.65
Qwen3-8B	QVQ-Max	QWQ-Max	84.52	90.80
QWQ-Max	QVQ-Max	Qwen3-8B	84.63	90.86
QWQ-Max	QVQ-Max	QWQ-Max	**84.73**	**90.89**

(d)

# Initial Candidate	R@1	mAP
2	84.63	90.85
3	**84.73**	**90.89**
4	84.68	90.88
5	84.27	90.66

(e)

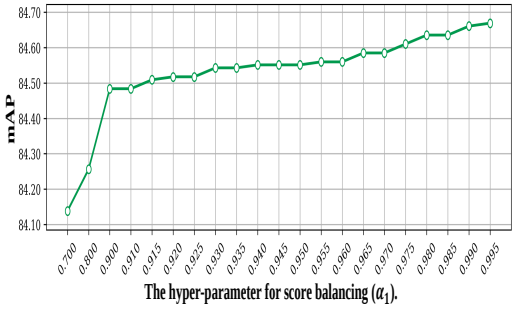

(f)

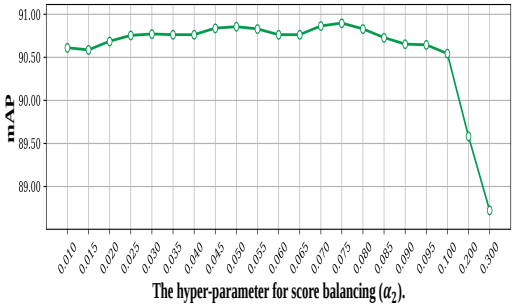

Qualitative Results. We present four qualitative examples of text-based person anomaly search (see Figure 4). For the first three cases (a-c), our method effectively retrieves the corresponding gallery images based on the query texts. In Figure 4(a), actions such as "waveing" and "fall" are critical. The cloze completion for the top-ranked gallery replaces "waveing" with "swinging," which is semantically similar, while other completions like "adjusting" are reasonable but less semantically aligned. However, for the action "fall," our method fails to predict accurate completions across all retrieved galleries because the ground truth image only show the tendency of an imminent fall. This process is visually similar to a leap. Similar patterns of partial semantic matches and occasional failures appear in Figure 4(b) and Figure 4(c). In Figure 4(d), our method does not retrieve the correct gallery image despite semantically matching completions in the top results. This is mainly due to the ambiguity in the query text, which presents a challenging scenario even for human annotators to identify the ground truth.

4.3 Ablation Studies and Further Discussion

Effect of primary components in our AnomalyLLM. We conduct ablation studies of primary components on the PAB dataset Yang et al. (2024b) with X^2VLM as the baseline (see Table 2(a)). In w cloze completion, we replace the comparison & re-ranking module with a similarity comparison module. Specifically, we use all-MiniLM-L6-v2 Galli et al. (2024) to embed completions and the text query into a 384-dimensional vector space, compute cosine similarity between embeddings of

completions and the text query, and re-rank completions accordingly. In w re-ranking, we treat cloze generation and completion as a single module, which is replaced by prompting the LMM to focus on object actions and colors while generating captions for images in the initial ranking list. Using the cloze generation and completion module, w cloze completion attains $+0.35\%$ Recall@1 accuracy. Applying the comparison & re-ranking module, w re-ranking achieves a $+0.46\%$ Recall@1 accuracy. Incorporating both modules, our full method achieves a $+0.96\%$ Recall@1 accuracy. These results show the effectiveness of the proposed components.

Effect of the weighting strategies in comparing and re-ranking. We conduct ablation studies on weighting strategies that convert descending ranking orders to corresponding descending scores (see Table 2(b)). Two strategies are evaluated: exponential and linear decay. For exponential decay, β ranges from 0.70 to 0.20, with β 0.50 achieving the best performance of 84.73% Recall@1 and 90.89 mAP accuracy. For linear decay, step sizes d range from -0.30 to -0.10, with step size -0.20 performing best among linear decays, achieving 84.73% Recall@1 and 90.88 mAP accuracy, slightly below the best exponential result.

Effect of the choice of LLMs and LMMs in cloze generation, cloze completion, and comparing and re-ranking. We conduct the ablation study on the choice of LLMs in different steps of our method (see Table 2(c)). For cloze generation, we choose from Qwen3-8B and QWQ-Max. These two LLMs achieve similar performance, with QWQ-Max producing more reliable clozes for subsequent steps in our method and achieving 84.73% Recall@1 and 90.89 mAP accuracy. For cloze completion, we choose among Qwen2.5-VL-7B, Qwen2.5-VL-3B, and QVQ-Max. We observe that LMMs with reasoning capability (QVQ-Max) outperform those without it. Specifically, QVQ-Max achieves the best performance, while Qwen-VL-3B and Qwen-VL-7B deliver comparable results, *i.e.*, 84.22%, 84.13%, and 90.65, 90.62 for Recall@1 and mAP, respectively. These findings show the importance of reasoning ability in cloze completion. For comparing and re-ranking, we choose among Qwen2.5-3B, Qwen2.5-7B, Qwen3-8B, and QWQ-Max. We find similar results that LLMs with reasoning capability have a better performance than LLMs without reasoning. QVQ-Max and Qwen3-8B achieve similarly strong performance, arriving at 84.52%, 84.73%, and 90.80, 90.89 for Recall@1 and mAP, respectively. We consider that both LLMs effectively leverage the embedded world knowledge within the model to perform semantically equivalent comparisons among cloze completions. On the other hand, smaller-capacity LLMs without reasoning capability, such as Qwen2.5-3B, exhibit poorer performance of 83.67% Recall@1 and 90.37 mAP. We attribute this to their reliance on lexical-level comparisons of cloze completions. Due to the inherent diversity and ambiguity of natural language, these models tend to treat completions with similar meanings but different wording as distinct from the text query. Consequently, they often produce trivial or even incorrect ranking results, assigning equal ranks to different completions (*i.e.*, completion 1 = completion 2).

Effect of the candidate number of the initial ranking list. We conduct an ablation study on the candidate number of the initial ranking list (see Table 2(d)). Among the lengths of 2, 3, 4, and 5, re-ranking with a candidate list length of 3 achieves the best performance. Using lengths of 2 or 4 leads to a slight drop in performance, while increasing the length to 5 results in a further decline to 84.27% Recall@1, 90.66 mAP. These results suggest that a moderate initial list length of 3 provides a good balance between covering ground-truth candidates and reducing noise or ambiguity introduced by larger candidate sets.

Effect of hyper-parameters in score balancing. We present ablation results on the hyper-parameters employed in score balancing, namely α_1 and α_2 (see Table 2(e) and Table 2(f)). In Table 2(e), with α_2 fixed at 1, increasing α_1 from 0.700 to 0.995 generally improves retrieval performance. Specifically, the mAP improves from 84.14 to 84.48 as α_1 increases from 0.700 to 0.900, and continues to rise gradually, saturating at 84.66 when α_1 is in the range of 0.910 to 0.995. In Table 2(f), with α_1 fixed at 1, varying α_2 from 0.010 to 0.300 initially causes fluctuations in mAP, which peaks at 90.89 mAP when $\alpha_2 = 0.075$, followed by a sharp decline to below 89.00 mAP when α_2 exceeds 0.100. These findings suggest that the first-stage score plays a crucial role in establishing a strong retrieval baseline, while the second-stage score contributes beneficial corrections within an appropriate range.

5 CONCLUSION

In this work, we present AnomalyLMM, the first framework to adapt Large Multi-modal Models (LMMs) for text-based person anomaly search. To address the challenges of fine-grained cross-modal alignment and anomaly recognition under sparse samples, our method introduces a novel coarse-to-fine pipeline and training-free adaptation strategies to bridge generative knowledge with discriminative retrieval. In particular, we are inspired by the cloze completion task to harness both LLM and LMM. We argue that only the ground-truth image could provide the visual cues to generate the most accurate verb and color words, while others are challenging to fill such cloze questions. In this way, we narrow down the search space and validate the top candidates. Extensive experiments on the PAB benchmark validate significant improvements over competitive baselines, while qualitative analysis validates the interpretability of our anomaly-behavior alignment. In the future, we will continue to study the response to the anomaly events, providing the evidence to support the decision, and generate the decision suggestions.

Limitations and Future Work. While AnomalyLMM advances the field, its performance inherently depends on the capabilities of underlying LMMs, inheriting their limitations in fine-grained visual-language understanding. As LMMs evolve (*e.g.*, with improved spatiotemporal reasoning or larger-scale anomaly-centric pretraining), our framework stands to benefit directly, potentially achieving further gains in robustness and generalization. Future directions include integrating dynamic anomaly memory banks and exploring few-shot adaptation to address rare behaviors. We hope this work inspires broader exploration of LMMs for safety-critical discriminative tasks.

Looking forward, AnomalyLMM opens promising directions for intelligent surveillance in smart city ecosystems. First, the framework could be extended to dynamic multi-camera environments, enabling real-time anomaly detection across urban infrastructures (*e.g.*, transportation hubs or crowded events) with natural language queries. Second, integrating domain-specific knowledge (*e.g.*, traffic rules or crowd behavior patterns) may enhance anomaly reasoning for public safety applications. Third, coupling with decision-support systems could enable proactive responses, such as alerting authorities or triggering emergency protocols, when detecting critical anomalies like unattended objects or violent behaviors. We also plan to investigate federated learning paradigms to address privacy concerns in city-scale deployments. By advancing the synergy between LMMs and surveillance intelligence, this work takes a step toward more interpretable and actionable anomaly analysis for next-generation urban computing.

REFERENCES

Gpt-4v(ision) system card. 2023. URL `https://api.semanticscholar.org/CorpusID:263218031`.

Josh Achiam, Steven Adler, Sandhini Agarwal, Lama Ahmad, Ilge Akkaya, Florencia Leoni Aleman, Diogo Almeida, Janko Altenschmidt, Sam Altman, Shyamal Anadkat, et al. Gpt-4 technical report. *ARXIV*, 2023.

Jean-Baptiste Alayrac, Jeff Donahue, Pauline Luc, Antoine Miech, Iain Barr, Yana Hasson, Karel Lenc, Arthur Mensch, Katherine Millican, Malcolm Reynolds, et al. Flamingo: a visual language model for few-shot learning. *NeurIPS*, 35:23716–23736, 2022.

Galen Andrew, Raman Arora, Jeff Bilmes, and Karen Livescu. Deep canonical correlation analysis. In *ICML*, pp. 1247–1255, 2013.

Yang Bai, Min Cao, Daming Gao, Ziqiang Cao, Chen Chen, Zhenfeng Fan, Liqiang Nie, and Min Zhang. Rasa: Relation and sensitivity aware representation learning for text-based person search. *ARXIV*, 2023.

Joya Chen, Zhaoyang Lv, Shiwei Wu, Kevin Qinghong Lin, Chenan Song, Difei Gao, Jia-Wei Liu, Ziteng Gao, Dongxing Mao, and Mike Zheng Shou. Videollm-online: Online video large language model for streaming video. In *CVPR*, pp. 18407–18418, 2024a.

Zhe Chen, Jiannan Wu, Wenhai Wang, Weijie Su, Guo Chen, Sen Xing, Muyan Zhong, Qinglong Zhang, Xizhou Zhu, Lewei Lu, et al. Internvl: Scaling up vision foundation models and aligning for generic visual-linguistic tasks. In *CVPR*, pp. 24185–24198, 2024b.

Soham Deshmukh, Benjamin Elizalde, Rita Singh, and Huaming Wang. Pengi: An audio language model for audio tasks. *NeurIPS*, 36:18090–18108, 2023.

Xinfeng Dong, Huaxiang Zhang, Xiao Dong, and Xu Lu. Iterative graph attention memory network for cross-modal retrieval. *Knowledge-Based Systems*, 226:107138, 2021.

Fartash Faghri, David J. Fleet, Jamie Ryan Kiros, and Sanja Fidler. VSE++: improving visual-semantic embeddings with hard negatives. In *BMVC*, pp. 12, 2018.

Carlo Galli, Nikolaos Donos, and Elena Calciolari. Performance of 4 pre-trained sentence transformer models in the semantic query of a systematic review dataset on peri-implantitis. *Information*, 15(2):68, 2024.

Satya Krishna Gorti, Noël Vouitsis, Junwei Ma, Keyvan Golestan, Maksims Volkovs, Animesh Garg, and Guangwei Yu. X-pool: Cross-modal language-video attention for text-video retrieval. In *CVPR*, pp. 5006–5015, 2022.

Jie Gui, Tuo Chen, Jing Zhang, Qiong Cao, Zhenan Sun, Hao Luo, and Dacheng Tao. A survey on self-supervised learning: Algorithms, applications, and future trends. *IEEE TPAMI*, 2024.

Mahmudul Hasan, Jonghyun Choi, Jan Neumann, Amit K Roy-Chowdhury, and Larry S Davis. Learning temporal regularity in video sequences. In *CVPR*, pp. 733–742, 2016.

Weizhen He, Yiheng Deng, Shixiang Tang, Qihao Chen, Qingsong Xie, Yizhou Wang, Lei Bai, Feng Zhu, Rui Zhao, Wanli Ouyang, et al. Instruct-reid: A multi-purpose person re-identification task with instructions. In *CVPR*, pp. 17521–17531, 2024.

Edward J Hu, Yelong Shen, Phillip Wallis, Zeyuan Allen-Zhu, Yuanzhi Li, Shean Wang, Lu Wang, Weizhu Chen, et al. Lora: Low-rank adaptation of large language models. *ICLR*, 1(2):3, 2022.

Zhong Ji, Kexin Chen, and Haoran Wang. Step-wise hierarchical alignment network for image-text matching. In Zhi-Hua Zhou (ed.), *IJCAI*, pp. 765–771, 2021.

Junnan Li, Dongxu Li, Silvio Savarese, and Steven Hoi. Blip-2: Bootstrapping language-image pre-training with frozen image encoders and large language models. In *ICML*, pp. 19730–19742, 2023.

Haotian Liu, Chunyuan Li, Qingyang Wu, and Yong Jae Lee. Visual instruction tuning. *NeurIPS*, 36:34892–34916, 2023.

Ziyu Liu, Zeyi Sun, Yuhang Zang, Wei Li, Pan Zhang, Xiaoyi Dong, Yuanjun Xiong, Dahua Lin, and Jiaqi Wang. Rar: Retrieving and ranking augmented mllms for visual recognition. *ARXIV*, 2024.

Ilya Loshchilov and Frank Hutter. Decoupled weight decay regularization. In *ICLR*, 2019.

Jiwen Lu, Junlin Hu, and Jie Zhou. Deep metric learning for visual understanding: An overview of recent advances. *IEEE Signal Processing Magazine*, 34(6):76–84, 2017.

Muhammad Maaz, Hanoona Rasheed, Salman Khan, and Fahad Shahbaz Khan. Video-chatgpt: Towards detailed video understanding via large vision and language models. *ARXIV*, 2023.

Ke Niu, Haiyang Yu, Mengyang Zhao, Teng Fu, Siyang Yi, Wei Lu, Bin Li, Xuelin Qian, and Xiangyang Xue. Chatreid: Open-ended interactive person retrieval via hierarchical progressive tuning for vision language models. *ARXIV*, 2025.

Alec Radford, Jong Wook Kim, Chris Hallacy, Aditya Ramesh, Gabriel Goh, Sandhini Agarwal, Girish Sastry, Amanda Askell, Pamela Mishkin, Jack Clark, et al. Learning transferable visual models from natural language supervision. In *ICML*, pp. 8748–8763, 2021.

Robin Rombach, Andreas Blattmann, Dominik Lorenz, Patrick Esser, and Björn Ommer. High-resolution image synthesis with latent diffusion models. In *CVPR*, pp. 10684–10695, 2022.

Xuankun Rong, Wenke Huang, Jian Liang, Jinhe Bi, Xun Xiao, Yiming Li, Bo Du, and Mang Ye. Backdoor cleaning without external guidance in mllm fine-tuning. *ARXIV*, 2025.

Franco Scarselli, Marco Gori, Ah Chung Tsoi, Markus Hagenbuchner, and Gabriele Monfardini. The graph neural network model. *IEEE TNNLS*, 20(1):61–80, 2008.

Xingyu Shen, Xiang Zhang, Xun Yang, Yibing Zhan, Long Lan, Jianfeng Dong, and Hongzhou Wu. Semantics-enriched cross-modal alignment for complex-query video moment retrieval. In *ACM MM*, pp. 4109–4118, 2023.

Waqas Sultani, Chen Chen, and Mubarak Shah. Real-world anomaly detection in surveillance videos. In *CVPR*, pp. 6479–6488, 2018.

Jintao Sun, Hao Fei, Gangyi Ding, and Zhedong Zheng. From data deluge to data curation: A filtering-wora paradigm for efficient text-based person search. In *WWW*, pp. 2341–2351, 2025.

Wentan Tan, Changxing Ding, Jiayu Jiang, Fei Wang, Yibing Zhan, and Dapeng Tao. Harnessing the power of mllms for transferable text-to-image person reid. In *CVPR*, pp. 17127–17137, 2024.

Shu Wang and Zhenjiang Miao. Anomaly detection in crowd scene. In *ICSPP*, pp. 1220–1223, 2010.

Tianshi Wang, Fengling Li, Lei Zhu, Jingjing Li, Zheng Zhang, and Heng Tao Shen. Cross-modal retrieval: a systematic review of methods and future directions. *Proceedings of the IEEE*, 2025.

Shengqiong Wu, Hao Fei, Leigang Qu, Wei Ji, and Tat-Seng Chua. Next-gpt: Any-to-any multimodal llm. In *ICML*, 2024.

An Yang, Baosong Yang, Beichen Zhang, Binyuan Hui, Bo Zheng, Bowen Yu, Chengyuan Li, Dayiheng Liu, Fei Huang, Haoran Wei, Huan Lin, Jian Yang, Jianhong Tu, Jianwei Zhang, Jianxin Yang, Jiaxi Yang, Jingren Zhou, Junyang Lin, Kai Dang, Keming Lu, Keqin Bao, Kexin Yang, Le Yu, Mei Li, Mingfeng Xue, Pei Zhang, Qin Zhu, Rui Men, Runji Lin, Tianhao Li, Tianyi Tang, Tingyu Xia, Xingzhang Ren, Xuancheng Ren, Yang Fan, Yang Su, Yichang Zhang, Yu Wan, Yuqiong Liu, Zeyu Cui, Zhenru Zhang, and Zihan Qiu. Qwen2.5 technical report. *ARXIV*, 2024a.

Shuyu Yang, Yinan Zhou, Zhedong Zheng, Yaxiong Wang, Li Zhu, and Yujiao Wu. Towards unified text-based person retrieval: A large-scale multi-attribute and language search benchmark. In *ACM MM*, pp. 4492–4501, 2023.

Shuyu Yang, Yaxiong Wang, Li Zhu, and Zhedong Zheng. Beyond walking: A large-scale image-text benchmark for text-based person anomaly search. *ARXIV*, 2024b.

Yuan Yao, Tianyu Yu, Ao Zhang, Chongyi Wang, Junbo Cui, Hongji Zhu, Tianchi Cai, Haoyu Li, Weilin Zhao, Zhihui He, et al. Minicpm-v: A gpt-4v level mllm on your phone. *ARXIV*, 2024.

Yan Zeng, Xinsong Zhang, and Hang Li. Multi-grained vision language pre-training: Aligning texts with visual concepts. In *ICML*, pp. 25994–26009, 2022.

Yan Zeng, Xinsong Zhang, Hang Li, Jiawei Wang, Jipeng Zhang, and Wangchunshu Zhou. X^{2}2-vlm: All-in-one pre-trained model for vision-language tasks. *IEEE TPAMI*, 46(5): 3156–3168, 2024.

Jiarui Zhang, Mahyar Khayatkhoei, Prateek Chhikara, and Filip Ilievski. Mllms know where to look: Training-free perception of small visual details with multimodal llms. *ICLR*, 2025.

Xin Zhang, Wen Xie, Ziqi Dai, Jun Rao, Haokun Wen, Xuan Luo, Meishan Zhang, and Min Zhang. Finetuning language models for multimodal question answering. In *ACM MM*, pp. 9420–9424, 2023.

Zhedong Zheng, Liang Zheng, and Yi Yang. A discriminatively learned cnn embedding for person reidentification. *ACM TOMM*, 14(1):1–20, 2017.

Zhedong Zheng, Liang Zheng, Michael Garrett, Yi Yang, Mingliang Xu, and Yi-Dong Shen. Dual-path convolutional image-text embeddings with instance loss. *ACM TOMM*, 16(2):1–23, 2020.

Kaiyang Zhou, Jingkang Yang, Chen Change Loy, and Ziwei Liu. Learning to prompt for vision-language models. *IJCV*, 130(9):2337–2348, 2022.